REVIEW ARTICLE

Lü-bi DENG

Theory of atom optics: Feynman's path integral approach (Ⅱ)

Abstract In the preceding paper, we discussed eight configurations of particle Fraunhofer diffraction. In this paper, we consider nine configurations of particle Fresnel diffraction, and have derived the wave functions of particles in these configurations. Furthermore, the author presents a new inertial navigator principle. Its devised accuracy is not lower than that of the inertial navigator based on cold atom interferometer. The new inertial navigator is named as ABSE inertial navigator. ABSE is abbreviation for Aharonov-Bohm-Sagnac effect.

Keywords atom optics, path integral

PACS numbers 42.50.Vk, 03.65.Db

1 Introduction

The theory of atom optics can be used in different approaches to research different problems. The present theory of atom optics is used in the following different approaches to study atomic diffraction and interference: (1) using formulas in classical optics [1–4], (2) from the time-independent Schrödinger equation to Kirchoff diffraction integral via Helmholtz equation [5], (3) solving Schrödinger equation or density matrix equation using superposition states [6–9], (4) path integral approach [10, 11], and (5) synthetic approach [5, 12]. The common properties of the above mentioned theories are the following: (1) they do not give atom probability distribution formulas on the screen; (2) most people only calculate phase differences from the action. This is an estimate, not exact results, because they only calculate phase difference between two classical paths; (3) complex computation [13]; (4) is a classical calculation [10] or numerical simulation [11]. The reasons are that they (except Refs. [13] and [11]) do not make quantum calculation. That is, superposition of probability amplitude is not calculated. Atom optics theory should be based on quantum mechanics, not based on classical optics. Thus, the atom optics theory has not been built systematically.

We use wave function to describe atomic quantum state. The wave function contains information about the internal state and the external motion of the atoms. For atomic diffraction and interference, an elegant approach is to express the wave function as a path integral and sum over all possible paths between the source and the observation point.

In the preceding paper [14], we discussed eight configurations of particle Fraunhofer diffraction. Here, we consider nine configurations of particle Fresnel diffraction.. These configurations are: (1) single slit, (2) single slit with van der Waals interaction, (3) double-slit, (4) grating, (5) rectangular aperture, (6) circular aperture, (7) Aharonov-Bohm effect of charged particle, (8) Aharonov-Bohm-Sagnac effect of charged particles (named as ABSE), and (9) straight edge. Besides these nine configurations, we also discuss the Aharonov-Bohm-Sagnac effect of Fraunhofer diffraction. We obtained the wave functions of particles in the above mentioned configurations.

Lü-bi DENG (✉)

Physics Department, Southeast University, Nanjing 210096, China
E-mail: lbdeng@seu.edu.cn

2 Fresnel single slit diffraction

Let an atom move from a source point S passing a single slit of width a to a point P on a screen (see Fig. 1). The time it takes the particle to run from S to C is denoted by t, and
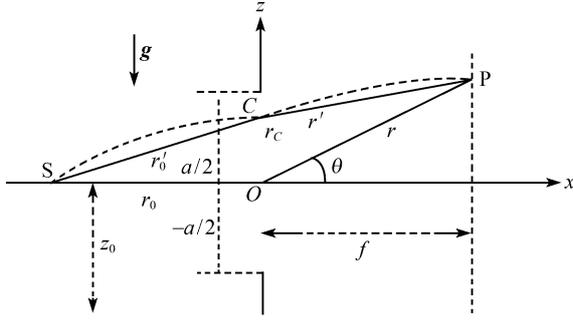
from S to P is denoted by *T*.

Fig. 1 Fresnel single-slit diffraction in the gravitation field.

Using Eq. (1) in Ref. [14], the wave function of atoms passing through a single slit can be rewritten as

$$\Psi(\boldsymbol{r},T) = \int_0^T \mathrm{d}t \int_C \mathrm{d}\boldsymbol{r}_C U(\boldsymbol{r}',T;\boldsymbol{r}_C,t)U(\boldsymbol{r}_C,t;\boldsymbol{r}_0,0) \tag{1}$$

where propagators [15]

$$U(\boldsymbol{r}_C,t\ ;\boldsymbol{r}_0,0) = \left(\frac{m}{\mathrm{i}ht}\right)^{3/2} \exp\left\{\frac{\mathrm{i}}{\hbar}\left[\frac{mr_0'^2}{2t} - \frac{mgt(z_C + |z_0|)}{2}\right.\right.$$
$$\left.\left. - \frac{mg^2t^3}{24}\right]\right\} \tag{2}$$

$$U(\boldsymbol{r},T\ ;\boldsymbol{r}_C,t) = \left(\frac{m}{\mathrm{i}h(T-t)}\right)^{3/2} \cdot \exp\left\{\frac{\mathrm{i}}{\hbar}\left[\frac{mr'^2}{2(T-t)}\right.\right.$$
$$\left.\left. - \frac{mgt(z + z_C)}{2} - \frac{mg^2(T-t)^3}{24}\right]\right\} \tag{3}$$

where *m* is the mass of the particle, *g* is the acceleration of gravity, z_0 is the height from the earth's surface, and *h* is Planck's constant. Using Fresnel approximation:

$$(r_0' + \boldsymbol{r}')^2 = (r_0 + f)^2 + 2(r_0 + f)\frac{(z - z_0)^2 + (y - y_0)^2}{2f} \tag{4}$$

we obtain the wave function of the atom Fresnel single-slit diffraction:

$$\Psi(\boldsymbol{r},T) = \left(\frac{m}{\mathrm{i}h}\right)^{5/2} \frac{(1+\mathrm{i})v\lambda f}{2r_0r\sqrt{T}} \exp\left\{\frac{\mathrm{i}}{\hbar}\left[\frac{1}{2}mv^2T\right.\right.$$
$$\left.\left. - \frac{mgT(z + |z_0|)}{2} - \frac{mg^2T^3}{12} - \frac{m^2g^2T^2\lambda f}{2h} - mgTz\right]\right\}$$
$$\cdot [F(\mu_2) - F(\mu_1)] \tag{5}$$

where $v = (r_0 + r)/T$ is average velocity of the particle. $\lambda = h/(mv)$ is average wavelength of the particle.

$$F(\mu_2) - F(\mu_1) = C(\mu_2) - C(\mu_1) + \mathrm{i}[S(\mu_2) - S(\mu_1)] \tag{6}$$

where $C(\mu)$ and $S(\mu)$ are Fresnel integrals:

$$C(\mu) = \int_0^\mu \cos\frac{\pi t^2}{2}\mathrm{d}t \tag{7}$$

$$S(\mu) = \int_0^\mu \sin\frac{\pi t^2}{2}\mathrm{d}t \tag{8}$$

where

$$\mu_2 = \sqrt{\frac{2}{\lambda f}}\left(z + \frac{a}{2}\right) + \sqrt{2\lambda f}\,\frac{mgT}{h} \tag{9}$$

$$\mu_1 = \sqrt{\frac{2}{\lambda f}}\left(z - \frac{a}{2}\right) + \sqrt{2\lambda f}\,\frac{mgT}{h} \tag{10}$$

Atom intensity distribution on the screen is an absolute square of the wave function $\Psi(\boldsymbol{r},T)$. Comparing our theoretical curves (*solid lines*) with the experimental curves (*dot lines*) [16] shown in Fig. 2, we find that they are in agreement with each other.
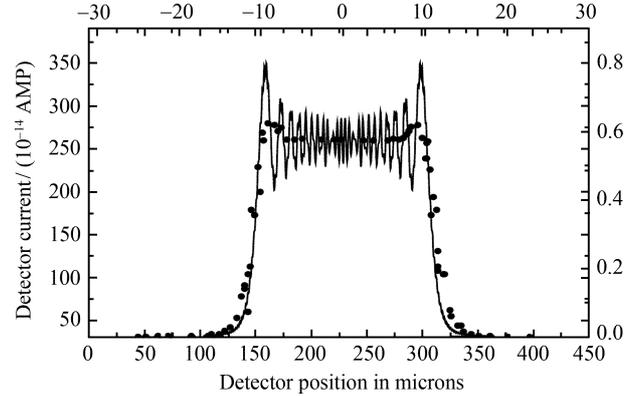

Fig. 2 Fresnel single slit diffraction.

3   Fresnel rectangular aperture diffraction

Using the above-mentioned method, we obtain a wave function of the state of atoms passing through a rectangular aperture of width *a* and length *b* on the screen in the gravitational field:

$$\Psi(\boldsymbol{r},T) = \left(\frac{m}{\mathrm{i}h}\right)^{5/2} \frac{(1+\mathrm{i})v\lambda f}{2r_0r\sqrt{T}} \exp\left\{\frac{\mathrm{i}}{\hbar}\left[\frac{1}{2}mv^2T\right.\right.$$
$$\left.\left. - \frac{mgT(z + |z_0|)}{2} - \frac{mg^2T^3}{12} - \frac{m^2g^2T^2\lambda f}{2h} - mgTz\right]\right\}$$
$$\cdot [F(\nu_2) - F(\nu_1)][F(\mu_2) - F(\mu_1)] \tag{11}$$

where

$$F(\nu) = C(\nu) + \mathrm{i}S(\nu) \tag{12}$$

$$\nu_2 = \sqrt{\frac{2}{\lambda f}}\left(y + \frac{b}{2}\right), \quad \nu_1 = \sqrt{\frac{2}{\lambda f}}\left(y - \frac{b}{2}\right) \tag{13}$$

and

$$F(\mu) = C(\mu) + iS(\mu)$$

$$\mu_2 = \sqrt{\frac{2}{\lambda f}}\left(z + \frac{a}{2}\right) + \sqrt{2\lambda f}\,\frac{mgT}{h} \tag{14}$$

$$\mu_1 = \sqrt{\frac{2}{\lambda f}}\left(z - \frac{b}{2}\right) + \sqrt{2\lambda f}\,\frac{mgT}{h} \tag{15}$$

4 Fresnel circular aperture diffraction

Using the above-mentioned method, we obtain a wave function of the state of atoms passing through a circular aperture of radius a on the screen in the gravitational field:

$$\Psi(\boldsymbol{r},T) = \left(\frac{m}{ih}\right)^{5/2}\frac{a^2 v}{2r_0 r\sqrt{T}}\exp\left\{\frac{i}{\hbar}\left[\frac{1}{2}mv^2T\right.\right.$$
$$\left.\left. - \frac{mgT(z + |z_0|)}{2} - \frac{mg^2 T^3}{12} + \frac{mv(z^2 + y^2)}{2f}\right]\right\}$$
$$\cdot\left[C(\kappa_1,\kappa_2) + iS(\kappa_1,\kappa_2)\right] \tag{16}$$

where

$$C(\kappa_1,\kappa_2) = \frac{\cos\left(\frac{1}{2}\kappa_1\right)}{\frac{1}{2}\kappa_1}U_1(\kappa_1,\kappa_2)$$
$$+ \frac{\sin\left(\frac{1}{2}\kappa_1\right)}{\frac{1}{2}\kappa_1}U_2(\kappa_1,\kappa_2) \tag{17}$$

$$S(\kappa_1,\kappa_2) = \frac{\sin\left(\frac{1}{2}\kappa_1\right)}{\frac{1}{2}\kappa_1}U_1(\kappa_1,\kappa_2)$$
$$- \frac{\cos\left(\frac{1}{2}\kappa_1\right)}{\frac{1}{2}\kappa_1}U_2(\kappa_1,\kappa_2) \tag{18}$$

where

$$\kappa_1 = \frac{a^2 k}{f}, \quad \kappa_2 = ka\sin\theta + \frac{mgTa}{\hbar} \tag{19}$$

U_1 and U_2 are Lommel functions.

5 Fresnel single-slit diffraction with van der Waals interaction

Taking the van der Waals interaction into account, after

adding an action $S = V\tau$, Eq. (1) becomes [14]

$$\Psi(\boldsymbol{r},T) = \int_0^T dt \int_C d\boldsymbol{r}_C U(\boldsymbol{r}',T;\boldsymbol{r}_C,t)e^{-iV\tau/\hbar}U(\boldsymbol{r}_C,t;\boldsymbol{r}_0,0) \tag{20}$$

where the van der Waals potential is $V = -C_3/l^3$, l is atom distance from the solid surface, C_3 is the potential constant, τ is the time that elapsed when an atom passes through the slit. Integrating Eq. (20), we obtain

$$\Psi(\boldsymbol{r},T) = \left(\frac{m}{ih}\right)^{5/2}\frac{-(1+i)v}{r_0 r\sqrt{T}}\sqrt{\frac{\lambda f}{2}}\exp\left\{\frac{i}{\hbar}\left[\frac{1}{2}mv^2T\right.\right.$$
$$\left.\left. - \frac{mgT(z + |z_0|)}{2} - \frac{mg^2 T^3}{12} - \frac{m^2 g^2 T^2 \lambda f}{2h} - mgTz\right]\right\}$$
$$\times\left\{\sqrt{\frac{\lambda f}{2}}\left[F(\mu_2) - F(\mu_1)\right] + \sum_{n=1}^{\infty}\frac{(iC)^n}{n!}\right.$$
$$\times\int_{-a/2}^{a/2}\frac{dz_C}{\left(1 - \frac{|z_C|}{d}\right)^{3n}}\exp\left\{i\frac{\pi}{2}\left[\sqrt{\frac{2}{\lambda f}}(z - z_C)\right.\right.$$
$$\left.\left.\left. + \sqrt{2\lambda f}\,\frac{mgT}{h}\right]^2\right\}\right\} \tag{21}$$

6 Fresnel diffraction at straight edge

Using the above-mentioned method, we obtain a wave function of atom Fresnel diffraction at straight edge in the gravitational field:

$$\Psi(\boldsymbol{r},T) = \left(\frac{m}{ih}\right)^{5/2}\frac{(1+i)v\lambda f}{2r_0 r\sqrt{T}}\exp\left\{\frac{i}{\hbar}\left[\frac{1}{2}mv^2T\right.\right.$$
$$\left.\left. - \frac{mgT(z + |z_0|)}{2} - \frac{mg^2 T^3}{12} - \frac{m^2 g^2 T^2 \lambda f}{2h} - mgTz\right]\right\}$$
$$\cdot\left[F\left(\sqrt{\frac{2}{\lambda f}}y\right) - F(-\infty)\right] \tag{22}$$

7 Fresnel double-slit diffraction

Atom Fresnel double-slit diffraction is shown in Fig. 3. Using the above-mentioned method, we obtain a wave function of atom Fresnel double-slit diffraction in the gravitational field:

$$\Psi(\boldsymbol{r},T) = \left(\frac{m}{ih}\right)^{5/2}\frac{(1+i)v\lambda f}{2r_0 r\sqrt{T}}\exp\left\{\frac{i}{\hbar}\left[\frac{1}{2}mv^2T\right.\right.$$
$$\left.\left. - \frac{mgT(z + |z_0|)}{2} - \frac{mg^2 T^3}{12} - \frac{m^2 g^2 T^2 \lambda f}{2h} - mgTz\right]\right\}$$

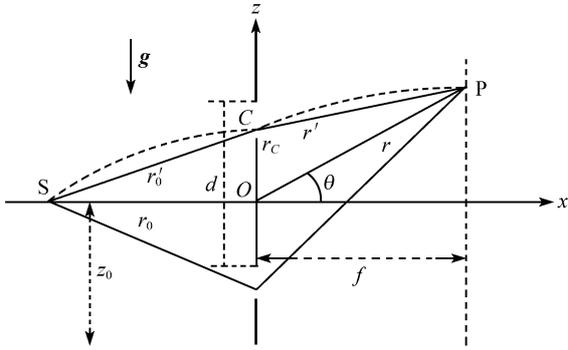$$\cdot [F(\mu_{21}) - F(\mu_{11})][F(\mu_{22}) - F(\mu_{12})] \qquad (23)$$

Fig. 3   Fresnel double-slit diffraction in the gravitation field.

where

$$\mu_{11} = \sqrt{\frac{2}{\lambda f}} \left[z - \frac{1}{2}(d+a) \right] + \sqrt{2\lambda f}\,\frac{mgT}{h} \qquad (24)$$

$$\mu_{21} = \sqrt{\frac{2}{\lambda f}} \left[z + \frac{1}{2}(d-a) \right] + \sqrt{2\lambda f}\,\frac{mgT}{h} \qquad (25)$$

$$\mu_{12} = \sqrt{\frac{2}{\lambda f}} \left[z + \frac{1}{2}(d-a) \right] + \sqrt{2\lambda f}\,\frac{mgT}{h} \qquad (26)$$

$$\mu_{22} = \sqrt{\frac{2}{\lambda f}} \left[z + \frac{1}{2}(d+a) \right] + \sqrt{2\lambda f}\,\frac{mgT}{h} \qquad (27)$$

a is the single slit width and d is the distance between two slits.

8   Fresnel grating diffraction

Using the above-mentioned method, we obtain a wave function of atom Fresnel grating diffraction in the gravitational field:

$$\Psi(\boldsymbol{r},T) = \left(\frac{m}{ih}\right)^{5/2} \frac{(1+i)v\lambda f}{2r_0 r \sqrt{T}} \exp\left\{ \frac{i}{\hbar} \left[\frac{1}{2} mv^2 T \right. \right.$$
$$\left. \left. - \frac{mgT(z+|z_0|)}{2} - \frac{mg^2 T^3}{12} - \frac{m^2 g^2 T^2 \lambda f}{2h} - mgTz \right] \right\}$$
$$\cdot \sum_{n=(1-N)/2}^{(N-1)/2} \left[F(\mu_{2n}) - F(\mu_{1n}) \right] \qquad (28)$$

where N is odd. When N is even, we may obtain the similar formula, in Eq. (28),

$$\mu_{1n} = \sqrt{\frac{2}{\lambda f}} \left[z - \frac{1}{2}\left(nd + \frac{a}{2} \right) \right] + \sqrt{2\lambda f}\,\frac{mgT}{h} \qquad (29)$$

$$\mu_{2n} = \sqrt{\frac{2}{\lambda f}} \left[z - \frac{1}{2}\left(nd - \frac{a}{2} \right) \right] + \sqrt{2\lambda f}\,\frac{mgT}{h} \qquad (30)$$

9   Aharonov-Bohm effect of Fresnel diffraction

The Aharonov-Bohm effect of Fresnel diffraction of the charged particle in the gravitational field is shown in Fig. 4. The symbol "⊙" in the figure expresses a tiny solenoid located between the two slits which we designed so that a magnetic field perpendicular to the plane of the figure can be produced in its interior. Using the above-mentioned method, we obtain a wave function of Aharonov-Bohm effect of Fresnel diffraction of the charged particle in the gravitational field:
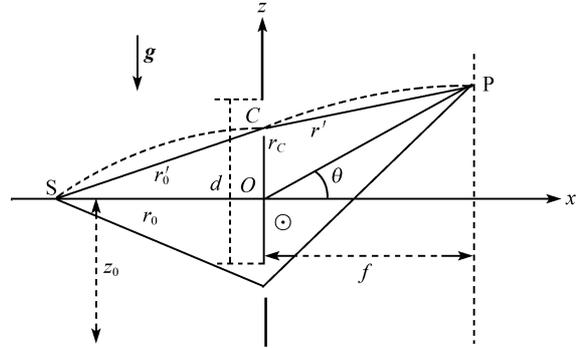

Fig. 4   Aharonov-Bohm effect of Fresnel diffraction.

$$\Psi(\boldsymbol{r},T) = \left(\frac{m}{ih}\right)^{5/2} \frac{(1+i)v\lambda f}{2r_0 r \sqrt{T}} \exp\left\{ \frac{i}{\hbar} \left[\frac{1}{2} mv^2 T \right. \right.$$
$$- \frac{mgT(z+|z_0|)}{2} - \frac{mg^2 T^3}{12} - \frac{m^2 g^2 T^2 \lambda f}{2h} - mgTz$$
$$\left. \left. - \frac{q}{2} \int_{SC_1 P} \boldsymbol{A} \cdot d\boldsymbol{r} - \frac{q}{2} \int_{SC_2 P} \boldsymbol{A} \cdot d\boldsymbol{r} \right] \right\}$$
$$\cdot \left\{ [F(\nu_{21}) - F(\nu_{11})] \exp\left(\frac{iq\Phi}{2\hbar} \right) \right.$$
$$\left. \cdot [F(\mu_{22}) - F(\mu_{12})] \exp\left(-\frac{iq\Phi}{2\hbar} \right) \right\} \qquad (31)$$

where $\boldsymbol{A}$ is the vector potential, q is the charge of the charged particle, Φ is the magnetic flux, $SC_1 P$ is the path from S to P along upper slit, and $SC_2 P$ is the path from S to P along the lower slit.

10   Aharonov-Bohm-Sagnac effect of Fresnel diffraction

In the Mach-Zehnder-type particle interferometer, if the inter-

ferometer is rotating with angular velocity Ω, around an axis through the center and perpendicular to the plane of the interferometer, using the above-mentioned method, we obtain a wave function of Aharonov-Bohm-Sagnac effect of Fresnel diffraction of the charged particle in the gravitational field:

$$
\begin{aligned}
\Psi(\boldsymbol{r},T) = & \left(\frac{m}{\mathrm{i}h}\right)^{5/2} \frac{(1+\mathrm{i})v\lambda f}{2r_0 r\sqrt{T}} \exp\left\{\frac{\mathrm{i}}{\hbar}\left[\frac{1}{2}mv^2 T\right.\right. \\
& \left. -\frac{mgT(z+|z_0|)}{2} - \frac{mg^2 T^3}{12} - \frac{m^2 g^2 T^2 \lambda f}{2h} - mgTz \right. \\
& \left.\left. -\frac{q}{2}\int_{\mathrm{SC_1P}} \boldsymbol{A}\cdot\mathrm{d}\boldsymbol{r} - \frac{q}{2}\int_{\mathrm{SC_2P}} \boldsymbol{A}\cdot\mathrm{d}\boldsymbol{r} \right]\right\} \\
& \cdot\left\{\left[F(\nu_{21}) - F(\nu_{11})\right]\exp\left[\mathrm{i}\left(\frac{q\Phi}{2\hbar} - \frac{m\Omega\cdot\sigma}{\hbar}\right)\right] \right. \\
& \left. + \left[F(\mu_{22}) - F(\mu_{12})\right]\exp\left[-\mathrm{i}\left(\frac{q\Phi}{2\hbar} - \frac{m\Omega\cdot\sigma}{\hbar}\right)\right]\right\}
\end{aligned}
\quad (32)
$$

where σ is the area vector enclosed by two paths in the Mach-Zehnder-type particle interferometer.

11 Aharonov-Bohm-Sagnac effect of Fraunhofer diffraction and ABSE inertial navigator principle

Using the above-mentioned method, we obtain a wave function of Aharonov-Bohm-Sagnac effect (named as ABSE) of Fraunhofer diffraction of the charged particle in the gravitational field:

$$
\begin{aligned}
\Psi(\boldsymbol{r},T) = & \left(\frac{m}{\mathrm{i}h}\right)^{5/2} \frac{2av}{r_0 r\sqrt{T}} \exp\left\{\frac{\mathrm{i}}{\hbar}\left[\frac{1}{2}mv^2 T\right.\right. \\
& \left.\left. -\frac{mgT(z+|z_0|)}{2} - \frac{mg^2 T^3}{12}\right]\right\} \\
& \cdot\frac{\sin\left(\dfrac{mva\sin\theta}{2\hbar} + \dfrac{mgTa}{2\hbar}\right)}{\dfrac{mva\sin\theta}{2\hbar} + \dfrac{mgTa}{2\hbar}} \\
& \cdot\cos\left(\frac{mvd\sin\theta}{2\hbar} + \frac{mgTd}{2\hbar} - \frac{q\Phi}{2\hbar} + \frac{m\Omega\cdot\sigma}{\hbar}\right)
\end{aligned}
\quad (33)
$$

where

$$
\Phi = \oint \boldsymbol{A}\cdot\mathrm{d}\boldsymbol{r} \tag{34}
$$

is a magnetic flux. The condition of maximum value of the interference fringe intensity is

$$
d\sin\theta = (n - n_\mathrm{g} - n_\mathrm{Sag} + n_{AB})\lambda \tag{35}
$$

where λ is the wave length of the particle. $n = 0, \pm 1, \pm 2,$

$\cdots$, n_g, n_Sag and n_{AB} are number of fringe shifts due to gravity, Sagnac effect and Aharonov-Bohm effect, respectively.

$$
n_\mathrm{g} = \frac{m(g + \boldsymbol{a}\cdot\boldsymbol{e})Td}{h} \tag{36}
$$

where $\boldsymbol{e}$ is unit vector along the moving axis direction, and $\boldsymbol{a}$ is linear acceleration,

$$
n_\mathrm{Sag} = \frac{2m\Omega\cdot\sigma}{h} \tag{37}
$$

$$
n_{AB} = \frac{q\Phi}{h} \tag{38}
$$

The position of the maximum value of the fringe is

$$
z_n = (n - n_\mathrm{g} - n_\mathrm{Sag} + n_{AB})\frac{\lambda f}{d} \tag{39}
$$

Eq. (35) is the theoretical foundation of the ABSE inertial navigator. It expresses that when changing the carrier's angular velocity, acceleration or acceleration of gravity, interference fringe will shift. In contrast, the carrier's angular velocity, acceleration and acceleration of gravity can be computed by interference fringe shifts, respectively. This new ABSE inertial navigator integrates an internally collecting gyroscope, accelerator and gradiometer. Its devised accuracy is not lower than that of the inertial navigator based on cold atom interferometer.

12 Summary

In summary, we can conclude the following:

(1) Using Feynman's path integral approach, we have presented and established a new theoretical formulation of particle optics and explicitly give wave functions describing the state particles in the above 23 configurations (including the 8 configurations in Ref. [14]).

(2) Our formulas provide a unified explanation of the diffraction and interference patterns of particles in the above 23 configurations.

(3) We have presented a new ion inertial navigator principle—the ABSE inertial navigator principle. This new inertial navigator integrates an internally collecting gyroscope, accelerator and gradiometer. Its devised accuracy is not lower than that of the inertial navigator based on cold atom interferometer (detailed calculation will be published elsewhere).

(4) Our theoretic wave functions and corresponding intensity distribution formulas for particles need to be confirmed by more experiments.

References

1. C. Jönsson, Z. Physik, 1961, 161: 454
2. O. Catnal and J. Mlynek, Phys. Rev. Lett., 1991, 66: 2689
3. R.E.Grisenti, W. Schöllkopt, J. P. Toennies, G. C. Hegerfeldt, and T. Köhler, Phys. Rev. Lett., 1999, 83: 1755
4. J. F. Clauser and M. W. Reinsch, Appl. Phys. B, 1992, 54: 380
5. P. R. Berman, ed., Atom Interferometry, New York: Academic Press, 1997
6. S. M. Tan and D. F. Walls, Appl. Phys. B, 1992, 54: 434
7. D. F. Walls and G. J. Milburn, Quantum Optics, Springer-Verlag, 1995
8. M. Orszag, Quantum Optics, Springer-Verlag, 2000
9. P. Meystre, Atom Optics, New York: Academic Press, 2001
10. P. Storey and C. Cohen-Tannoudji, J. Phys. II, 1994, 4: 1999
11. M. Gondran and A. Gondran, Am. J. Phys., 2005, 73: 507
12. Ch. J. Bordé, Matter-wave Interferometers: A Synthetic Approach, in: M. Orszag, Quantum Optics, Springer-Verlag, 2000: 257
13. Ch. J. Bordé , Ch. Salomon, S. Avrillier, A. Van Lerberghe, and Ch. Bréant, Phys. Rev. A, 1984, 30: 1836
14. Lü-bi Deng, Front. Phys. China, 2006, 1 (1): 47
15. R. P. Feynman and A.-R.Hibbs, Quantum Mechanics and Path Integrals, New York: McGraw-Hill, 1965
16. J. A. Leavitt and F. A. Bills, Am. J. Phys., 1969, 37: 905